Concrete Strength in Tied Columns

by Shamim A. Sheikh, C. C. Yeh, and Shafik Khoury

Stress-strain curve of concrete in compression depends on several factors including the size and shape of compressed concrete, types and intensity of stresses acting in different directions on concrete elements, and the presence of strain gradient. The strength of concrete has little effect on the behavior of sections under pure flexure and under flexure and low-axial load levels. For sections subjected to flexure and large axial loads, when concrete strength significantly influences section behavior, it is believed that strength of concrete in the specimens is reduced with an increase in axial load level. Results from five 12 in. (305 mm) square and 9 ft (2.74 m) long column specimens are reported in this paper. Based on this and the results from previous research, a simple relationship is suggested in which the concrete strength is reduced from f'_c at the balanced load to $0.85f'_c$ for concentric compression. A second-degree parabolic stress-strain curve with strain at peak stress equal to 0.002 can be used for reasonably accurate and conservative prediction of section capacity.

In assessing the behavior of concrete sections, one of the basic assumptions is that the stress-strain curve for concrete defining the magnitude and distribution of compressive stress is known. Under pure flexure, the strength of concrete does not have a significant influence on the flexural capacity and deformation of a section. Under combined flexure and axial load, strength of concrete plays an important role in the determination of the section capacity, particularly when the axial load is large. The ACI Building Code[1] allows the use of any concrete stress-strain relationship in compression that predicts section strength in substantial agreement with the results of comprehensive tests. In lieu of a more accurate curve, a rectangular stress block of $0.85f'_c$ over an equivalent compression zone is permitted by the code. The depth of this compression zone is βc where c is the depth of the neutral axis. Up to $f'_c = 4000$ psi (27.6 MPa), β is assumed to be 0.85. For higher strength, β is reduced at a rate of .05 for each 1000 psi (6.9 MPa) in excess of 4000 psi (27.6 MPa). The lower limit on β is 0.65. The maximum extreme fiber concrete compressive strain is suggested to be 0.003. To accurately represent a parabolic stress-strain curve for concrete with f'_c and 0.002 as the coordinates of the

peak point, the dimensions of the rectangular stress block are $0.9f'_c$ and $0.833c$ for the extreme fiber strain of 0.003. The moment of the area about the baseline of the stress block calculated by using these dimensions is only slightly higher than the moment calculated from the stress block suggested by the ACI Building Code.

For the entire axial load-moment interaction curve, the concrete strength in the member is taken as f'_c except for the point corresponding to the pure axial load P_o for which the concrete strength is assumed to be equal to $0.85f'_c$. The change in the strength of concrete from f'_c to $0.85f'_c$ is rather sudden and lacks logic. Several reasons behind the lower strength of concrete in the column compared with f'_c have been advanced. Among these are the difference in specimen shape and size, sedimentation due to vertical casting of a column, and water gain at the top of the column. However, these reasons should not be applicable only to the case of concentric compression. There are several test results reported in the literature that deal with the members subjected to pure compression or tested under low axial load and flexure.[2-5] Results from the tests on specimens subjected to high axial load and flexure, however, are limited.[6,7] Since a part of the P-M interaction curve corresponding to high axial load is not used directly in the design due to the minimum eccentricity requirements of the code, this part of the curve has not received due attention. In the seismic design of structures where the members are subjected to extreme loads, the accurate prediction of their capacities in the high axial load regions becomes important. In addition, for the nonseismic design of members, the factor of safety against failure will also be affected if member capacities are not accurately known.

ACI member Shamim A. Sheikh is currently an associate professor of civil engineering at the University of Toronto. He is a member of ACI-ASCE Committees 441, Reinforced Concrete Columns; and 442, Response of Concrete Buildings to Lateral Forces. His research interests include confinement of concrete, earthquake resistance of reinforced concrete, and expansive cement concrete and its application in deep foundation.

ACI member C. C. Yeh is a former graduate student and research assistant at the University of Houston where he received his PhD in 1988. His research work concentrated on the behavior of confined concrete columns under high axial load and flexure.

ACI member Shafik Khoury is a research assistant and a graduate student of civil engineering at the University of Houston. He received his MS from Alexandria University in Egypt and is currently working toward his PhD in the area of confined concrete.
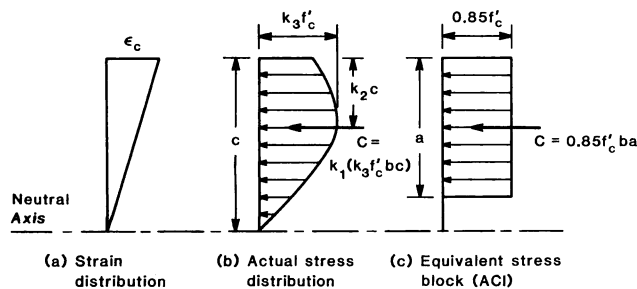
(a) Strain distribution (b) Actual stress distribution (c) Equivalent stress block (ACI)

Fig. 1—Stress and strain distributions in the compressive zone of a concrete section

Table 1 — Stress block parameters[8]

f'_c, psi	k_1	k_2	k_3
3000	0.82	0.46	0.97
4000	0.79	0.45	0.94
5000	0.75	0.44	0.92
6000	0.71	0.47	0.92
7000	0.67	0.41	0.93

1000 psi = 6.895 MPa.

BACKGROUND

The shape of the stress block on compressed concrete keeps changing as the moment on the section changes. The section reaches its maximum moment of resistance, i.e., flexural capacity, when the product of the total compressive force in the concrete and the internal lever arm is a maximum. The actual stress block and the equivalent rectangular stress distribution are shown in Fig. 1. For unconfined concrete, the most notable work to determine parameters k_1, k_2, and k_3 was conducted by Hognestad, Hanson, and McHenry.[2,8] The critical section of the plain concrete used in this test program was 5 in. (127 mm) wide and 8 in. (203 mm) deep. Two independent compressive loads were applied such that the neutral axis was maintained at one of the 5 in. (127 mm) faces of the specimen throughout the test. By comparing the internal and external actions, the parameters k_1, k_2, and k_3 were determined. Average values for these parameters for f'_c varying between 3000 and 7000 psi (20.7 and 48.3 MPa) are shown in Table 1.

It is important to note that k_3 values were less than 1.0 in all the cases and for most commonly used con-
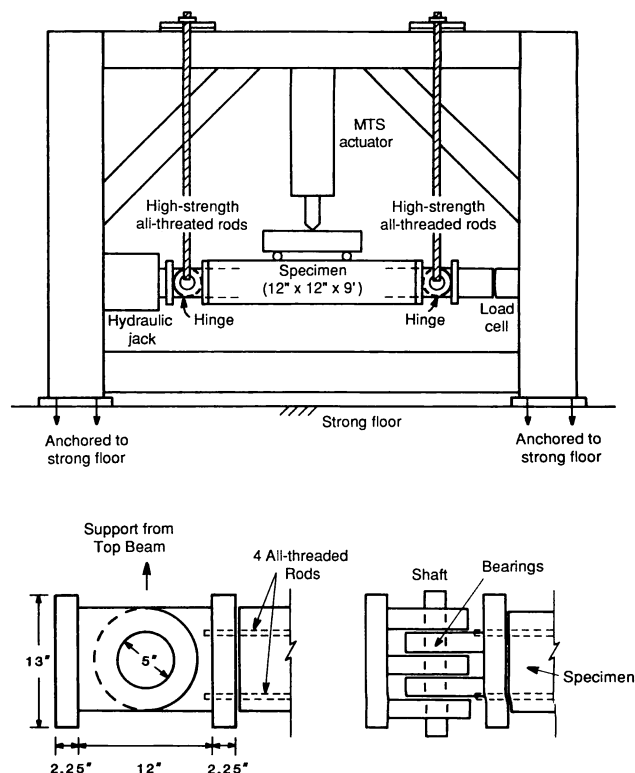

Fig. 2—Test setup and hinge details

crete strength, k_3 is approximately equal to 0.93. The strain profile in all these test specimens was such that the axial load level in a reinforced section would be larger than the balanced load. As mentioned earlier, it is generally accepted that under concentric compression, strength of concrete in a column is approximately equal to 0.85 f'_c. At large axial load levels, the strength of concrete in the member has significant effect on its section capacity. At and below the balanced load, the section capacity is relatively independent of the concrete strength.

CURRENT WORK

As part of a large experimental program, five columns were tested under flexure while simultaneously subjected to constant axial loads above the balanced level.[7] The specimens were subjected to a constant axial load first, followed by an application of third-point loads to create a shear-free test zone in the middle third of the column length. The test setup is shown in Fig. 2. At each end of the specimen, a hinge was attached with the help of four all-threaded bars embedded in concrete. The axis of rotation of the hinge was the centroidal axis of the shaft, which was also used to support the specimen from the upper beam of the test frame. This arrangement allowed the specimen to rotate freely at ends with minimal friction and at the same time allowed the mechanism of axial load application to remain undisturbed throughout the test. This facilitated the calculation of the applied moment without any need for complex corrections. Each hinge consisted of two parts connected by the shaft, as shown in Fig. 2. One part of the hinge contained two roller bearings, and the

Table 2 — Details of test specimens and results

| Specimen | f'_c, ksi | Lateral steel | | | | $\dfrac{P}{f'_c\,A_g}$ | $\dfrac{P_{all}}{f'_c\,A_g}$ | M_{max}, k-in. | $\dfrac{M_{max}}{M_1}$, | $\dfrac{M_{max}}{M_2}$, | $\dfrac{M_{max}}{M_3}$, | ϵ_c at M_{max} |
		Size	Spacing, in.	ρ_s, percent	f_{yh}, ksi							
E-8	3.76	#3	@ 5	0.84	70	0.78	0.74	1143	0.98	0.95	1.04	0.0022
A-11	4.05	6 mm	@ 4¼	0.77	68	0.74	0.72	1196	0.94	0.97	1.00	0.0038
F-12	4.85	6 mm	@ 3½	0.82	67	0.60	0.68	1425	0.91	0.98	0.96	0.0029
D-14	3.90	6 mm	@ 4¼	0.81	67	0.74	0.70	1031	0.90	1.01	0.97	0.0025
A-16	4.92	6 mm	@ 4¼	0.77	81	0.60	0.67	1393	0.88	0.95	0.93	0.0028

$P_{all} = 0.56\,[0.85\,f'_c\,(A_g - A_s) + A_s f_y]$.
1 ksi = 6.895 MPa.
1 in. = 25.4 mm.

E A F D

Fig. 3—Tie arrangements

Fig. 4—Stress-strain curves for longitudinal and lateral steel
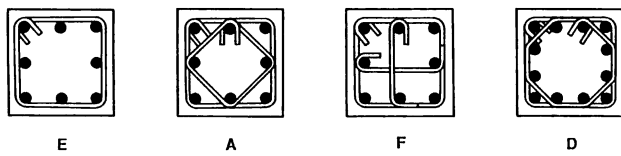
other part contained three roller bearings. Each bearing was capable of resisting more than 250 kips (1112 kN) of load, thus providing a hinge capacity in excess of 500 kips (2224 kN).

Details of specimens

All the specimens were 12 in. (305 mm) square and 9 ft (2.74 m) long. All the specimens contained eight No. 6 longitudinal steel bars except Specimen D-14, which contained twelve No. 5 longitudinal steel bars. Details of the specimens are given in Table 2. Total amount of lateral reinforcement was approximately the same in all the specimens, but four different tie arrangements, shown in Fig. 3, were used. The volumetric ratio of tie steel was approximately 50 percent of that required for seismic design in Appendix A of the ACI Building Code.[1] For nonseismic design, only No. 3 perimeter ties are required at 12 in. (305 mm) spacing according to the code provisions. This provides a lateral reinforcement volumetric ratio of 0.35 percent, considering that the size of the core measured from the centerline of tie steel was 10.5 in. (267 mm) square. All the specimens listed in Table 2, therefore, satisfy the general code provisions. Although the 6 mm diameter tie steel was deformed, the size of the bar is less than the minimum allowed by the code. The specimens can, therefore, be considered as two-thirds scale models of 18 in. square columns.

Normal weight concrete with ¾-in. (19 mm) maximum size aggregate was used. Compressive strength of concrete as measured from standard cylinders is listed in Table 2. The strain in concrete corresponding to the maximum stress varied between 0.00175 and 0.0022. The strength values reported in Table 2 were obtained from strength versus age relationship obtained for each batch of concrete based on the tests of cylinders conducted at regular intervals. At least three cylinders were tested at any one time. Grade 60 steel was used in all the specimens. Steel properties are shown in Fig. 4.

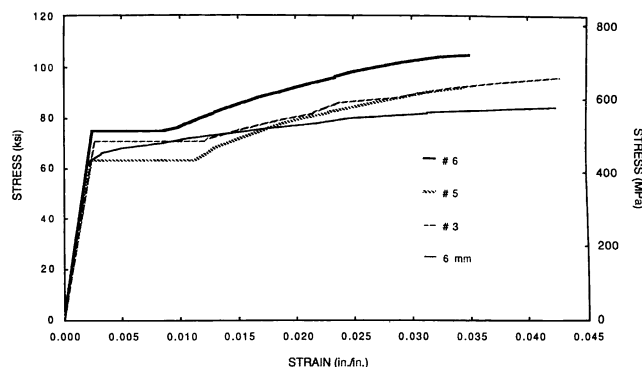All the specimens were cast horizontally. The distance between the longitudinal bars was constant in all

the specimens. The perimeter ties in all the specimens were anchored inside the core with 135 deg hooks at their ends. With the exception of Configuration E, middle bars in all the specimens were supported by tie bends. Crossties, with 180 deg hooks at one end and 90 deg hooks at the other, in Specimen F-12 were alternated as required in Appendix A of the ACI Building Code.

Test procedure

Before testing a specimen, the hinges were attached to its ends and the specimen was installed in the testing frame as shown in Fig. 2. A thin layer of Plaster of Paris was used between the hinges and the specimen. Axial load was applied with the help of a 1000 kip (4.5 MN) hydraulic jack and measured with a load cell of similar capacity. Alignment of the specimen was carried out by checking the deformation readings at every 40-kip (180-kN) interval while the axial load was increased to 200 kips (890 kN). After a satisfactory alignment was achieved in that load range, the axial load was increased to the maximum predetermined value. After a final check and any needed adjustments, the specimen was unloaded and all the instruments were reset for the test.

At the start of the test, the axial load was applied to a predetermined value that remained constant throughout the test. Readings from all the instruments were recorded at regular intervals during the application of the axial load with the help of a data acquisition system. The instrumentation included electrical resistance strain gages on longitudinal and lateral steel in the test region of the specimens. Longitudinal concrete strain in the core was measured by using LVDTs (linear variable
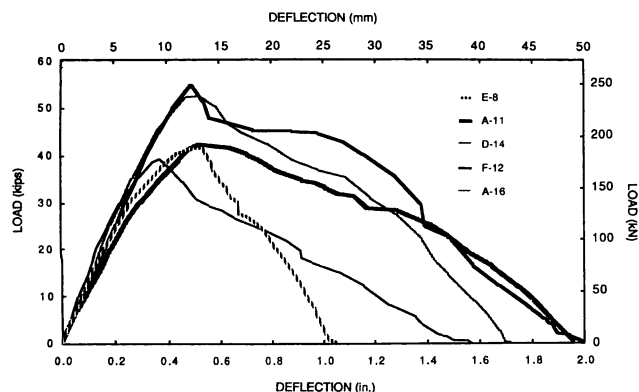
Fig. 5—Lateral load-versus-lateral deflection curves

Fig. 6—Moment-curvature curves

differential transformers) over a gage length of 10 in. (254 mm) at three locations along the section depth. All-threaded $\frac{5}{16}$ in. (8 mm) diameter embedded rods were used to install the LVDTs. In addition, the downward deflection was measured by LVDTs and dial indicators along the specimen length. Deflection in the lateral direction was also monitored by dial gages along the specimen length to prevent off-center axial loading.

Lateral load was applied with the help of a 146-kip (650-kN) actuator by controlling the displacement rate. For the ascending part of the load-displacement curves, the displacement rate was maintained at 0.04 to 0.05 in./min (1 to 1.25 mm/min). Beyond the peak point, the rate of displacement was reduced in some columns to avoid sudden failure and increased by a factor of 2 in. columns which showed ductile behavior. Readings from all the instruments were recorded at frequent intervals by holding the deformation constant for a few seconds. Tests were continued until after the lateral load dropped to zero on the descending parts of the curves. Most tests were completed in 3 hr.

RESULTS

The lateral load versus deflection curves for the five specimens are shown in Fig. 5. Before the peak lateral load, the axial load was maintained at the predetermined level with relative ease. At larger deformations, the axial load needed to be adjusted frequently.

The moment-curvature relations of all the specimens are shown in Fig. 6. In the initial stages of loading, most of the section moment was caused by the lateral load. At larger deformations, the secondary moment, a product of axial load and deflection, became the dominant part of the total section moment. Near the end of the test, when the lateral load approached zero, almost the entire moment was generated by axial load. At this stage, any attempt to maintain the axial load increased deflection of the specimen significantly. Since the moment cannot exceed the section capacity at that instance, the specimen maintained an axial load less than the original predetermined value. Level of axial load at this stage depended mainly on the confinement provided by the lateral reinforcement in the test zone of the specimen.
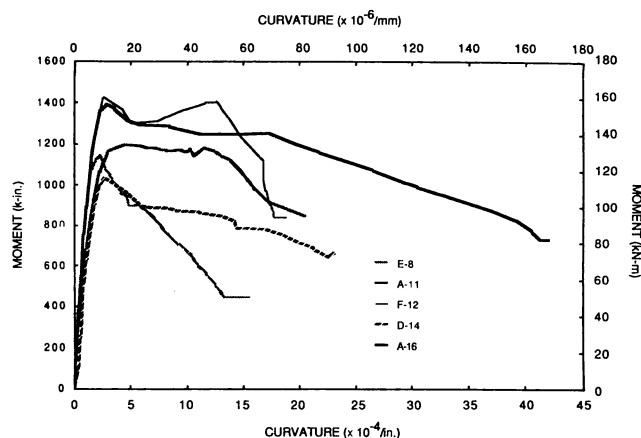
A comparison of various curves in Fig. 6 provides an evaluation of the effects of several variables. A detailed discussion on this aspect is available elsewhere.[7] Only a brief summary on the effects of the level of axial load, steel configuration, and the use of 90 deg hooks is presented here. A comparison of the behavior of Specimens F-12 and A-16 clearly indicates that 90 deg hooks are not capable of providing as effective a support to the longitudinal bars as the internal ties, thus resulting in reduced ductility of the section. Slightly higher strength in Specimen F-12 can be explained by the closer tie spacing in this specimen. Adverse effects of high axial load on section ductility can be observed by comparing curves for Specimens A-11 and A-16. The distribution of steel has a significant effect on the behavior of specimens, as is obvious from a comparison of Specimens E-8, A-11, and D-14. The specimen with unsupported bars (E-8) showed much less ductility compared with the specimens in which all the bars were laterally supported by tie bends.

Table 2 lists the maximum moment M_{max} experienced by each of the specimens, and the ratios between M_{max} and the theoretical moment capacities M_1, M_2, or M_3. Extreme fiber compressive strain values ϵ_c at the instant the specimens carried the maximum moment are also listed in Table 2. Crushing of cover concrete was observed to take place at a strain approximately equal to 0.00375 in most specimens. Capacity M_1 was based on second-degree parabolic stress-strain curves up to a strain of 0.003 with maximum stress equal to f_c' and the corresponding strain equal to 0.002. The theoretical capacity M_2 was determined based on the actual stress-strain curves of concrete cylinders. The strength of concrete was obtained from strength-versus-age relationships. It is obvious that there is a significant difference between M_1 and M_2 in most columns. The M_1 and M_2 values used in Table 2 were calculated at the extreme fiber compressive strain of 0.003. For M_2 values calculated at the extreme fiber compressive strain equal to 1.5 times the strain at peak stress, the M_{max}/M_2 ratios for the five columns were 1.02, 0.95, 0.97, 0.93, and 0.94, respectively. The capacity M_3 is based on the rectangular stress block suggested in the ACI Building Code.[1]
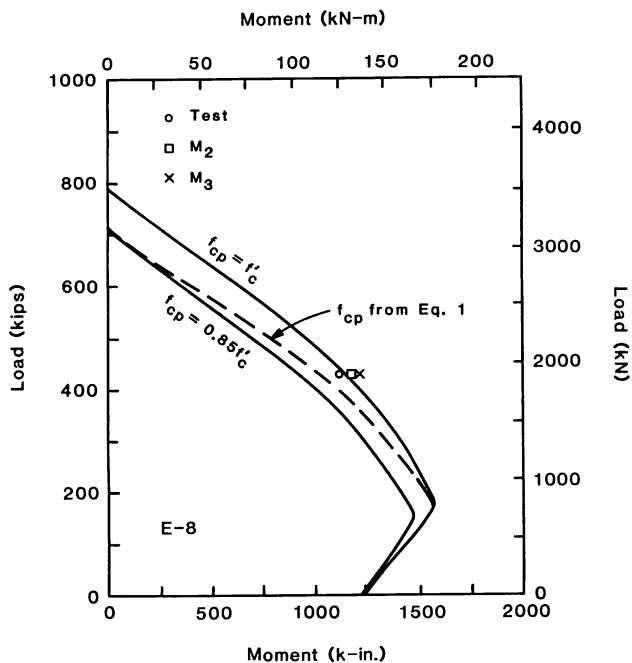
Fig. 7—Axial load-moment interaction curves for Specimen E-8

Fig. 8—Axial load-moment interaction curves for Specimen A-11

Fig. 9—Axial load-moment interaction curves for Specimen F-12

It is obvious that the experimental capacities are significantly lower than most of the theoretical capacities including those obtained from using the stress block suggested by the code. In this comparison, the lower of the two values of M_{max}/M_2, as discussed previously, should be used. The M_1 values are the commonly used theoretical capacities for reinforced and prestressed concrete sections.[9] The experimental capacities in comparison with the M_1 values are quite low, indicating that the strength of concrete in the specimens is probably overestimated.

The $P/f'_c Ag$ ratios are also compared with the ratios allowed by the ACI Building Code in Table 2. The applied axial load varied between 88 and 106 percent of the allowable load. It should be noted that the allowable load is only 56 percent of the axial load capacity of a section.

The test specimens in this study were cast horizontally; therefore, the maximum depth of concrete cast at one time was 12 in. (305 mm). The tests were performed such that the "top" concrete was subjected to extreme compressive strains. This may partially explain lower than expected strength of the section. In columns cast vertically, the effect of top concrete will even be more pronounced. This effect alone, however, does not explain the fact that lower than predicted moment capacities were obtained despite the confinement provided by the lateral steel. In addition, a trend was observed that the ratio between the section moment capacity and its theoretical capacity reduced with an increase in axial load.[7] An increase in axial load in a column tested under flexure has two effects. First, the strain gradient becomes less steep and may result in lower strength of concrete, i.e., the beneficial effects of strength gradient are reduced. Secondly, the neutral axis depth is increased, which will engage more bottom
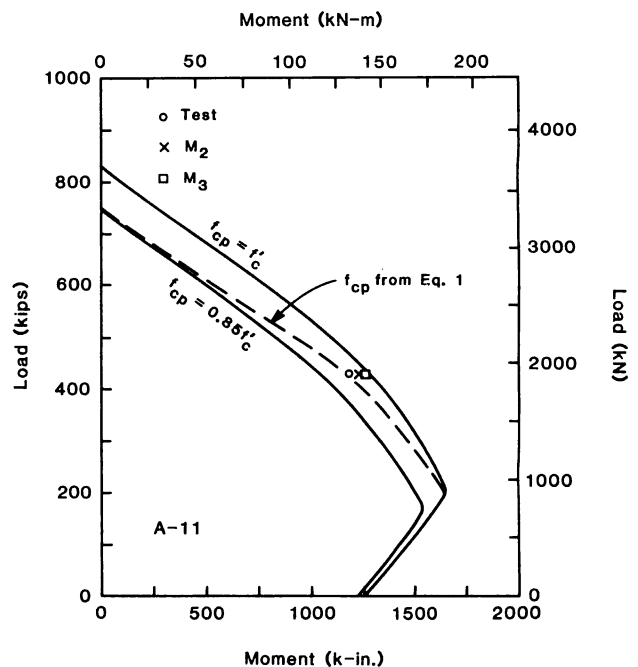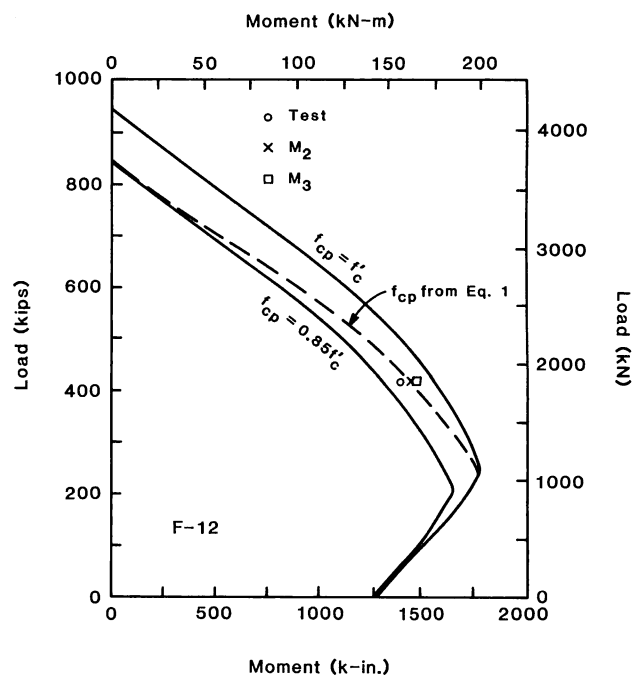
concrete but most likely will not have any effect on the section capacity because the failure will still be initiated in the top concrete.

Fig. 7 through 11 show the section P-M interaction curves for five columns based on M_1 values. Two curves are shown for each column, one with $f_{cp} = f'_c$ and the other with $f_{cp} = 0.85 f'_c$. A second-degree parabolic stress-strain curve for concrete in compression was used. The strain corresponding to the maximum stress was assumed to be 0.002. The moment capacity of the
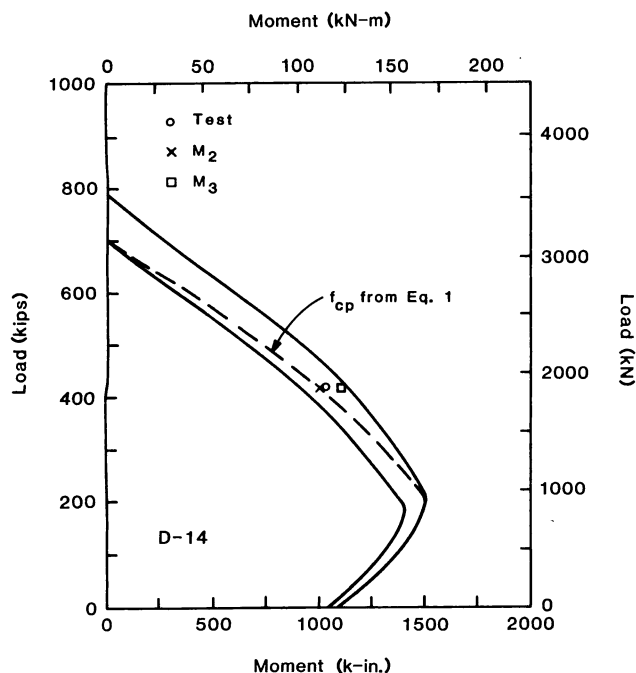
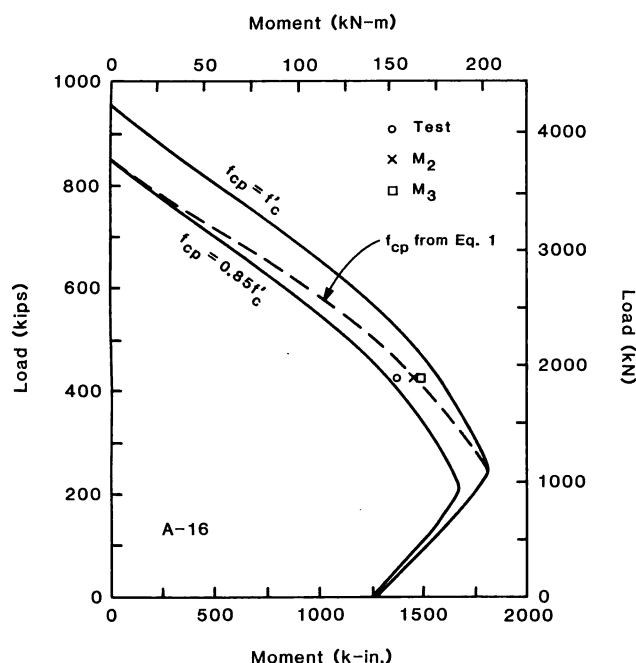Fig. 10—Axial load-moment interaction curves for Specimen D-14

Fig. 11—Axial load-moment interaction curves for Specimen A-16

Fig. 12—Typical axial load-moment interaction diagram for a reinforced concrete section

section was assumed to take place at an extreme fiber concrete strain of 0.003. The theoretical moment capacities obtained from using the actual stress-strain curves M_2 and from using the stress block suggested by the ACI Building Code (M_3) are also shown on the plots along with the experimental strength values. In most columns, the experimental points fall inside the outer curves, indicating that the theoretical strength envelope is on the unsafe side. Although the differences between the analytical and the experimental values are not very large, they cannot be explained on the basis of the ex-
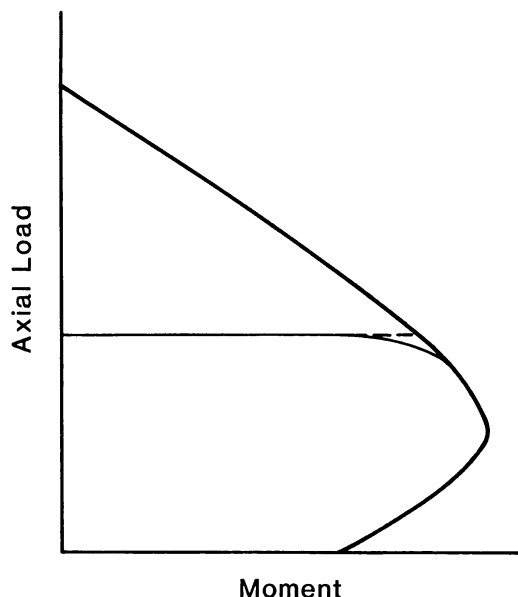
perimental error. In all the tests, axial loads were applied before the specimens were subjected to flexure. The path of loading is shown in Fig. 12. In the initial stages, it was easy to maintain the axial load, but at large deformations the axial load would drop below the fixed limit and had to be adjusted regularly. Since the amount of lateral reinforcement in the columns was not large enough to excessively increase the flexural capacity of the sections and produce very ductile behavior (Fig. 6), the probable path of loading would cross the capacity curve at an axial load value somewhat lower than the predetermined fixed value. The flexural capacity thus obtained experimentally would overestimate the actual capacity.

The lateral reinforcement in all the specimens would result in enhanced concrete strength and, hence, an increase in moment capacity. This enhancement in concrete strength may be as much as 20 percent in some specimens according to the available confinement models.[7,10,11] Considering this increase in the flexural capacity and the fact that the measured flexural strength may correspond to a lower axial load, the test values as shown in Fig. 7 through 11 appear better than they actually are. With the minimum required[1] amount of lateral steel, the difference between the experimental and the theoretical moment capacities may even be larger. Another factor that affects the section capacity is the separation between cover concrete and core concrete due to the layer of stirrup steel. With a reduced tie spacing, the cover concrete will spall off at a lower stress, resulting in a reduction in the section capacity. In the tests reported here, this phenomenon did not appear to have very significant effects. With the available experimental evidence, it is not possible to evaluate the effects of each of the previously discussed factors individually.

Data in Fig. 7 through 11 suggest that, for accurate analytical prediction of the section capacity, the

strength of concrete in the column should be reduced from f_c' to $0.85 f_c'$ as the axial load increases from balanced load P_b to pure axial load capacity P_o. In the columns that are reinforced with the minimum required[1] tie steel, the reduction may even be more severe. In the case of high axial load and low volumetric ratio of tie steel, concrete would be subjected to large tensile strains in the lateral direction before moment is applied. Vecchio and Collins[12] observed in their tests on concrete panels subjected to pure shear that when concrete was subjected to coexisting lateral tensile strains, its compressive strength was reduced. Although this does not provide a direct parallel to the problem at hand, it indicates that the state of stress in concrete before moment is applied and the type of strain gradient have significant effects on the concrete compressive strength. A simple relationship is suggested in Eq. (1) for the strength of concrete as a function of the axial load on the section

$$\text{For } P < P_b;\ f_{cp} = f_c'$$

$$\text{For } P_b < P < P_o;\ f_{cp} = f_c'\left(1 - 0.15\,\frac{P - P_b}{P_o - P_b}\right) \quad (1)$$

Test results from Hognestad's work[2] shown in Table 1 support the previous argument. Parameter k_3, which represents the ratio between f_{cp} and f_c' in these tests, had a value approximately equal to 0.93 for the commonly used concrete strength. As mentioned earlier, the strain profiles for these specimens corresponded to axial loads larger than the balanced loads. Interaction curves for the specimens based on Eq. (1) are also shown in Fig. 7 through 11. The agreement between the theoretical and experimental section capacities is quite good for all the specimens. However, more data points are needed to further validate the hypothesis presented here.

SUMMARY AND CONCLUSIONS

For the calculation of flexural capacity of a reinforced concrete section while subjected to an axial load larger than the balanced load, several stress-strain curves can be used including a rectangular stress block.[1] In the research reported here, experimental results from five 12 in. (305 mm) square, 9 ft (2.74 m) long columns are compared with the analytical results. It was observed that almost all the analytical capacity values overestimated the test capacities of the sections. The axial load on the specimens that remained constant throughout the tests varied between $0.6 f_c'\, Ag$ and $0.78 f_c'\, Ag$. The balanced load for these sections was in the vicinity of $0.37 f_c'\, Ag$.

It was concluded that the strength of concrete depends on strain gradient and the state of stress in concrete at ultimate. An increase in axial load results in a reduction in concrete strength. Below the balanced axial load level, the concrete strength does not have very significant influence on the flexural capacity of the sec-

tion. A small error in concrete strength would, therefore, not affect section strength. In this range, concrete strength equal to f_c' can be used to evaluate the section capacity. Above the balanced load level, a simple relationship is suggested that reduces concrete strength from f_c' at balanced load to $0.85 f_c'$ when the section is subjected to pure axial compression. In addition to the current test data, results from previous experimental studies confirm the previous phenomenon. A second-degree parabolic stress-strain curve for concrete under compression can be used with strain at peak stress equal to 0.002. The extreme fiber compressive strain of 0.003 provides a reasonably accurate prediction of the section capacity under flexure and axial load.

REFERENCES

1. ACI Committee 318, "Building Code Requirements for Reinforced Concrete (ACI 318-83)," American Concrete Institute, Detroit, 1983, 111 pp.

2. Hognestad, E., "A Study of Combined Bending and Axial Load in Reinforced Concrete Members," Bulletin No. 399, Engineering Experiment Station, University of Illinois, Urbana, 1951, 128 pp.

3. Saatcioglu, M., "Reinforced Concrete Columns Subjected to Uniaxial and Biaxial Load Reversals," Proceedings, 8th World Conference on Earthquake Engineering, San Francisco, 1984, V. 5, pp. 585-592.

4. Sheikh, Shamim A., and Uzumeri, S. M., "Strength and Ductility of Tied Concrete Columns," Proceedings, ASCE, V. 106, ST5, May 1980, pp. 1079-1102.

5. Soesianawati, M. T., "Limited Ductility Design of Reinforced Concrete Columns," Research Report No. 86-10, University of Canterbury, Christchurch, 1986, 208 pp.

6. Park, Robert; Priestley, M. J. Nigel; and Gill, Wayne D., "Ductility of Square-Confined Concrete Columns," Proceedings, ASCE, V. 108, ST4, Apr. 1982, pp. 919-950.

7. Yeh, C., and Sheikh, S., "Behavior of Confined Concrete Columns Under Axial Load and Flexure," Research Report No. UHCE88-2, University of Houston, 1988, 310 pp.

8. Hognestad, Eivind; Hanson, N. W.; and McHenry, Douglas, "Concrete Stress Distribution Ultimate Strength Design," ACI JOURNAL, Proceedings V. 52, No. 4, Dec. 1955, pp. 455-479.

9. Collins, M. P., and Mitchell, D. Prestressed Concrete Basics, Canadian Prestressed Concrete Institute, Ottawa, 1987, 614 pp.

10. Mander, J. B.; Priestley, M. J. N.; and Park, R., "Theoretical Stress-Strain Model for Confined Concrete," Journal of Structural Engineering, ASCE, V. 114, No. 8, Aug. 1988, pp. 1804-1826.

11. Sheikh, Shamim A., and Uzumeri, S. M., "Analytical Model for Concrete Confinement in Tied Columns," Proceedings, ASCE, V. 108, ST12, Dec. 1982, pp. 2703-2722.

12. Vecchio, Frank J., and Collins, Michael P., "The Modified Compression-Field Theory for Reinforced Concrete Elements Subjected to Shear," ACI JOURNAL, Proceedings V. 83, No. 2, Mar.-Apr. 1986, pp. 219-231.